

Draft

SLAC PUB-4579
3/23/88
(N)

Very High Luminosity e^+e^- Colliders
for b, c, Quark and tau-Lepton Physics

THE PEP OPTION

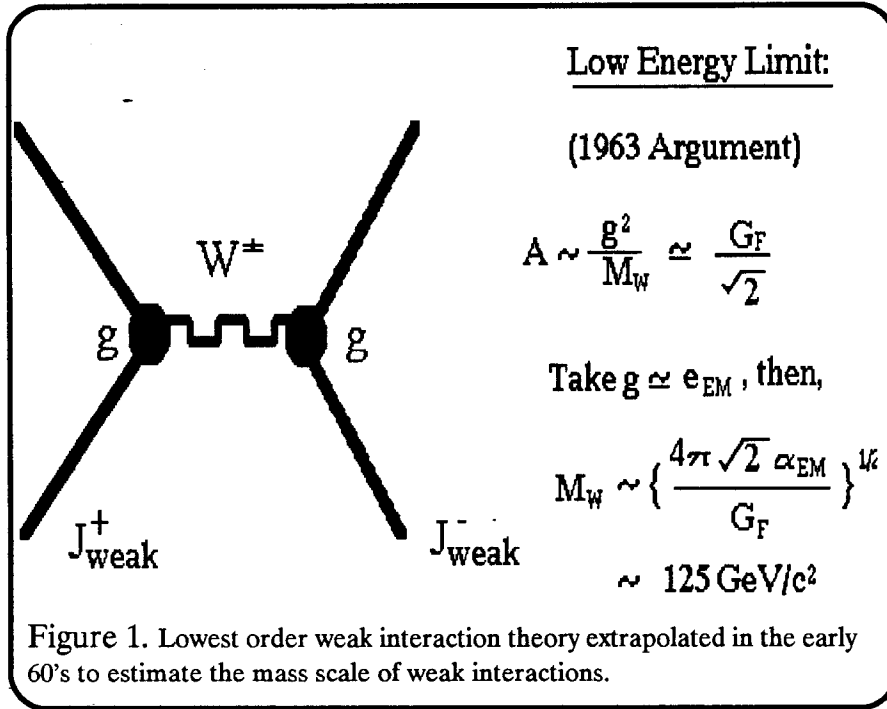
by
Elliott D. Bloom
Stanford Linear Accelerator Center,
Stanford University, Stanford, CA, 94309

Presented at the B-Meson Factory Workshop,
Stanford Linear Accelerator Center,
Stanford University, CA, 94309
September 7-8, 1987

Work supported by Department of Energy Contract # DE-AC003-76SF00515

1. Introduction and Motivation

How to learn about the “next” energy scale has been a major occupation of particle physicists over the past few years. The SSC is one such obvious attempt, though perhaps not the most imaginative one (and certainly not the most economical). A lesson from history may have relevance to this question. The weak interaction has been very helpful in determining the electroweak scale, as well as determining



the phenomenology of the electroweak interactions. Figure 1 reproduces one of the arguments, circa the early 1960's, which led to the conclusion that 100 GeV was the “natural” scale of the weak interaction. Extensive and frequently precision experiments at the available mass scale ($E_{cm}^{\infty} \sim 0.5\text{-}30 \text{ GeV}$) over the next 20 years, using a variety of techniques, then led to a firm prediction of the W and Z masses, detailed knowledge of their decays, and the relatively economical machine designed to observe them at CERN in the 80's. It is possible that history can repeat by using CP violation as a similar tool to explore the “next” mass scale.

The frame work which we now consider CP violation is the K-M matrix of the standard model with three quark-lepton generations. In this model, CP violation is the result of the one irreducible phase in the K-M matrix; indeed, three generations and the K-M matrix were developed in large part to provide an explanation of CP violation in the early 1970's. At the present time, there seem to be two possibilities: the mass scale of CP violation is electroweak, or the mass scale is much larger. If the relevant mass scale which correctly describes CP violation is on the order of the present electroweak scale, one expects large CP violations in the B-meson system explainable in the context of the K-M matrix. The ability to observe CP violation, if the standard model is correct, is considerably enhanced if the recent ARGUS collaboration results on B^0_d mixing are confirmed. ARGUS has obtained, ⁽¹⁾

$$X_d = \Delta M/\Gamma(B^0_d) = 0.78 \pm 0.16,$$

as compared to theoretical predictions in the range $X_d < 0.2$, ⁽²⁾

The mixing is calculated using the real part of the box diagram of figure 2, ⁽³⁾

$$\Delta M/\Gamma = (32\pi/3) \text{Re}\{V_{ub}V_{td}^*\}/|V_{cb}|^2 (B_B f_B^2 \eta_2 m_t^2/m_b^4).$$

The theoretical unknowns are the K-M matrix elements, V_{ub} and V_{td} , the B meson structure constant ($B_B^{1/2} f_B$), the QCD correction η_2 , and the mass of the top quark, m_t . The large ARGUS mixing result and the B-lifetime measurements ⁽⁴⁾ ($\sim 10^{-12}$ sec.) imply a larger than predicted V_{ub} , and smaller than

predicted V_{cb} , respectively, as well as $m_t > 50 \text{ GeV}$ ⁽⁵⁾ (just about the mass lower limit measured by UA-1 ⁽⁶⁾).

Experimental estimates of ϵ and ϵ' , from measurements of CP violation in the K^0 system ⁽⁷⁾, where,

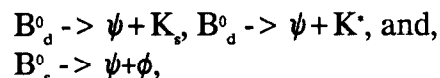
$$\eta_{\pm} \equiv \text{amp}(K_L \rightarrow \pi^+\pi^-) / \text{amp}(K_S \rightarrow \pi^+\pi^-) = \epsilon + \epsilon' = 2.279(26) \times 10^{-3} e^{i(44.6 \pm 1.2)},$$

and,

$$\eta_{00} \equiv \text{amp}(K_L \rightarrow \pi^0\pi^0) / \text{amp}(K_S \rightarrow \pi^0\pi^0) = \epsilon - 2\epsilon' = 2.29(4) \times 10^{-3} e^{i(55^\circ \pm 6^\circ)},$$

then imply a large K-M phase, $\delta \approx 100^\circ$. ⁽⁸⁾ Figure 3 shows the approximate values of s_2 , s_3 , and δ (K-M matrix representation) inferred from the experiments. ⁽⁸⁾

The large mixing, measured for B_d , and predicted for B_s , then implies an incredibly large CP violation in B decays, on the order of 10%-50%. ⁽⁵⁾ A striking manifestation of CP violation is predicted to be a large difference in time evolution between initially B^0 and \bar{B}^0 mesons as they decay into particular final states. The reactions,



look particularly accessible and promising for realizing a CP violation at this time.

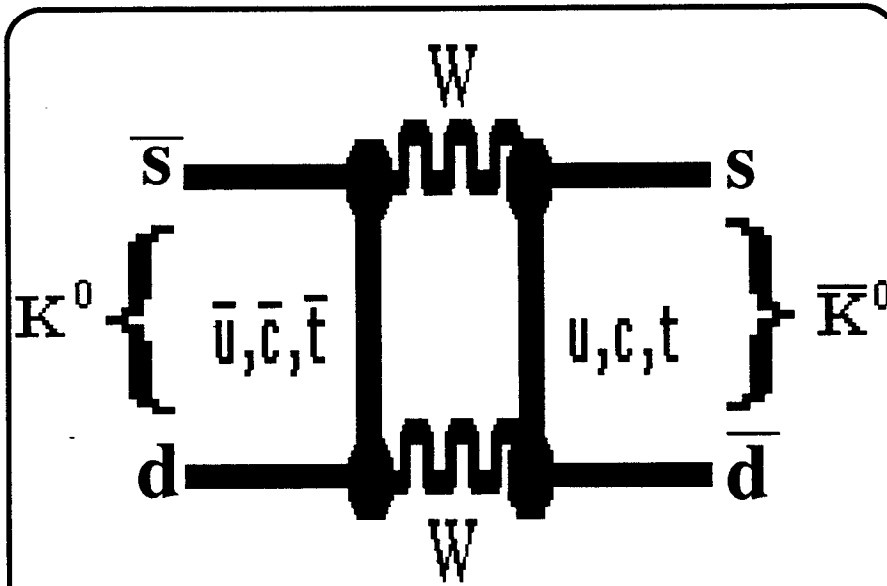


Figure 2. Second order box diagram used in the calculation of CP violation in the standard model.

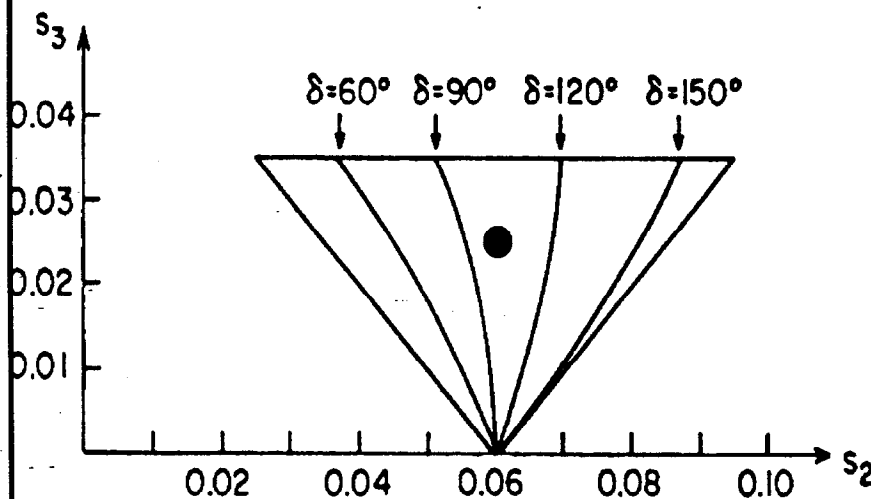


Figure 3. The allowed range of K-M parameters as determined using b-quark lifetime and leptonic branching ratio. The "best" value is somewhat loosely chosen at the dot.

What if the standard model is wrong? Then, there is probably a new mass scale and CP violation is its prophet. An example of such a model is the "minimal" left-right symmetric model involving a very heavy right handed W. ⁽⁹⁾ Figure 4 shows the box diagrams relevant to this model. Assume that box 1 $\equiv I$, is relatively real, and that the entire CP violation in the K^0 system is due to box 2. Note that only two generations are included in the calculation, and thus we are effectively assuming that K-M contributes nothing, or is irrelevant to CP violation ($\delta = 0$). In addition, we assume equal left and right handed Cabbibo angles. It can be shown, ⁽⁹⁾

$$\text{box2} = I \times [M(W_L)M(W_R)]^2 \times 430 \times e^{i\phi}$$

where $M(W_{L,R})$ are the left handed and right handed W masses, respectively, 430 is a numerical factor which depends on the detailed structure of the theory, and ϕ is a CP violating phase induced by right handed W exchange.

Assuming the entire CP violating effect is due to the diagrams of figure 4, we obtain, by comparing to experiment,

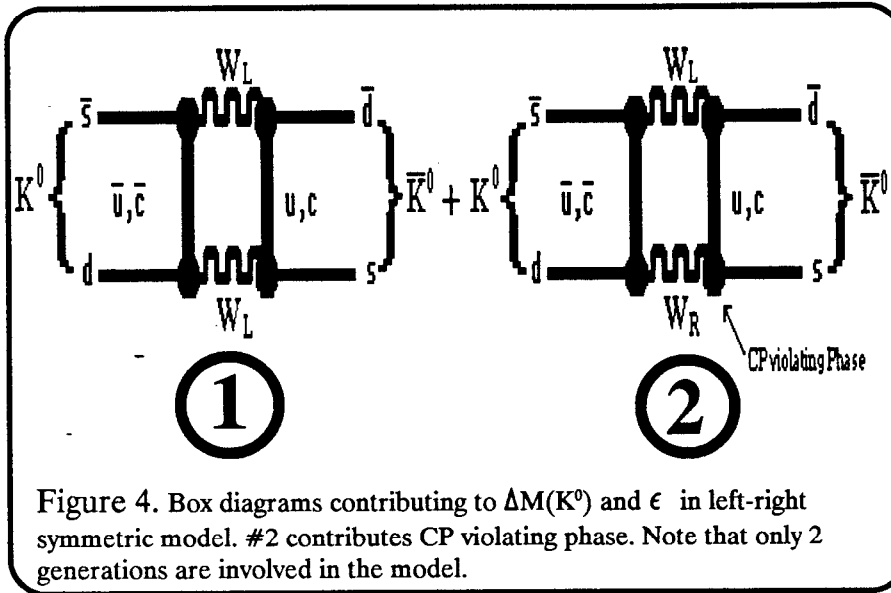


Figure 4. Box diagrams contributing to $\Delta M(K^0)$ and ϵ in left-right symmetric model. #2 contributes CP violating phase. Note that only 2 generations are involved in the model.

$$\Delta M_{LRS}(K^0) = \text{Re}\{\text{box2}\} = I \times [M(W_L)/M(W_R)]^2 \times 430 \times \cos\theta \leq \text{box1}$$

$$\epsilon_{LRS}(K^0) = \text{Im}\{\text{box2}\} = [M(W_L)/M(W_R)]^2 \times 430 / (2/2) \times \sin\theta = 2 \times 10^3.$$

These conditions imply that, $2 \text{ TeV} \leq W_R \leq 20 \text{ TeV}$.⁽⁹⁾ In this case, CP violation in the B system would be comparable to that in the K system as the B mass is still very small compared to $M(W_R)$. Very high precision CP violation experiments would then be needed in the B system, as they are now needed in the K system, to explore the source of the violation.

Both scenarios above promise many fruitful years of physics to come from a careful and systematic study of the B system, if a sufficient number of B decays are available. This last point, however, presents a severe challenge to the experimentalist.

2. Where to "B".

The question of which B meson sources, coupled with which detection techniques, looms as the major challenges in the future of B meson studies.⁽¹⁰⁾ There are two general areas of possibilities, proton machines and e^+e^- colliders. I will briefly discuss both sets of possibilities and then reflect in more detail on e^+e^- colliders, which is my area of specialization. Details for the proton machine option are give in B. Cox's talk at this workshop.⁽¹¹⁾

2a. Protons or Electrons

High energy proton machines, both fixed target and colliders, presently have some advantages as compared to e^+e^- colliders. First and most importantly, there exists the potential to produce very large numbers of B mesons per unit running time. As table 1 shows, up to 10^9 B's might be produced per day of running at the SSC, with lesser amounts from presently available machines. In addition, decay

	TeV II Few Years	TeV II Improved	TeV Coll Few Years	TeV Coll Improved	SSC
E_{cm} (GeV)	40	40	2000	2000	40,000
$\sigma(b\bar{b})/\sigma_{tot}$	10^{-6}	10^{-6}	10^{-4}	10^{-4}	10^{-3}
\mathcal{L}_{day} (pb^{-1})*	3	30	.03	.3	?
Interactions 200 days	10^{13}	10^{14}	10^{12}	10^{13}	10^{14}
#BB/200days	10^7	10^8	3×10^7	10^9	10^{11}
$\gamma\beta c\tau$ (mm)	7	7	2	2	3
$\langle n_{ch} \rangle_{detector}$	8	8	100	100	50
Solid angle	0.2π	0.2π	$\sim 4\pi$	$\sim 4\pi$	$\sim \pi$

* Approximate Lumi limit producing 10^7 interactions/sec Max. in some cases.

Table 1. Comparison of Hadronic Experiments

lengths for B's of a few mm may allow measurement of decay vertices with relative ease if radiation problems can be overcome. However, as is outlined in table 1, these potential advantages are presently all but neutralized by a number of disadvantages. Though $\sigma_{tot} \sim 50$ mb, $\sigma(b\bar{b})/\sigma_{tot}$ is very small and thus the $b\bar{b}$ events are very difficult to extract with reasonable efficiency (even in Monte Carlo land). The trigger will be crucial here. ⁽¹¹⁾ In addition, large multiplicities generated from the $b\bar{b}$ part of the event, coupled with many additional particles not associated with the $b\bar{b}$, exacerbate the problem of B finding. Finally, the question of radiation damage from high doses near the target (or I.P. for colliders) presents a severe technological challenge.

Presently, conceived advantages and disadvantages for e^+e^- colliders are essentially orthogonal to those for proton machines. Though detection of B's is not simple here, experience has shown that the $\sigma(b\bar{b})/\sigma_{tot} \sim 0.1 - .25$ makes the problem rather straight forward, and new detectors presently being built at Cornell, LEP and SLAC will improve matters considerably. As is shown in table 2, a small beam pipe radius is projected for a number of machines allowing improved lifetime measurements and flavor tagging. However, the question at e^+e^- colliders is rate. Figure 5 and table 2 illustrate the problem. Even at the peak of the Z^0 , where $\sigma_{bb} \sim 6nb$, rate is severely limiting. The problem is luminosity, or the lack thereof, for presently available or building e^+e^- colliders. It seems clear that if CP violation is to be explored by e^+e^- collider experiments, factors of 100-1000 in luminosity are needed over presently operating machines depending on E_{cm} and machine design, i.e., symmetric or non-symmetric beam energies. Table 1 shows projected operating luminosities for a number of machines. Some of these machines are well along, while others are just at the conceptual stage. Through state of the art and beyond, none of the machines in the table have the integrated luminosity to do anything but scratch the region of interesting limits on CP violation in the B system.

2b. Energy and Kinematics

Not only is the question of \mathcal{L} vs σ_{tot} , i.e., production rate, a crucial issue for e^+e^- colliders, E_{cm} and movement of the center of mass are also important. The latter points relate to the measurement of CP violation though the spectacular signature of unequal partial widths, i.e., decay length vs time for certain combinations of final states for B^0 vs \bar{B}^0 . For example, this phenomenon is predicted to occur for a CP self conjugate decay mode, f, common to B^0 and \bar{B}^0 , ⁽¹²⁾ and yields disparate time dependent partial widths for B^0 and $[\bar{B}^0]$ given by,

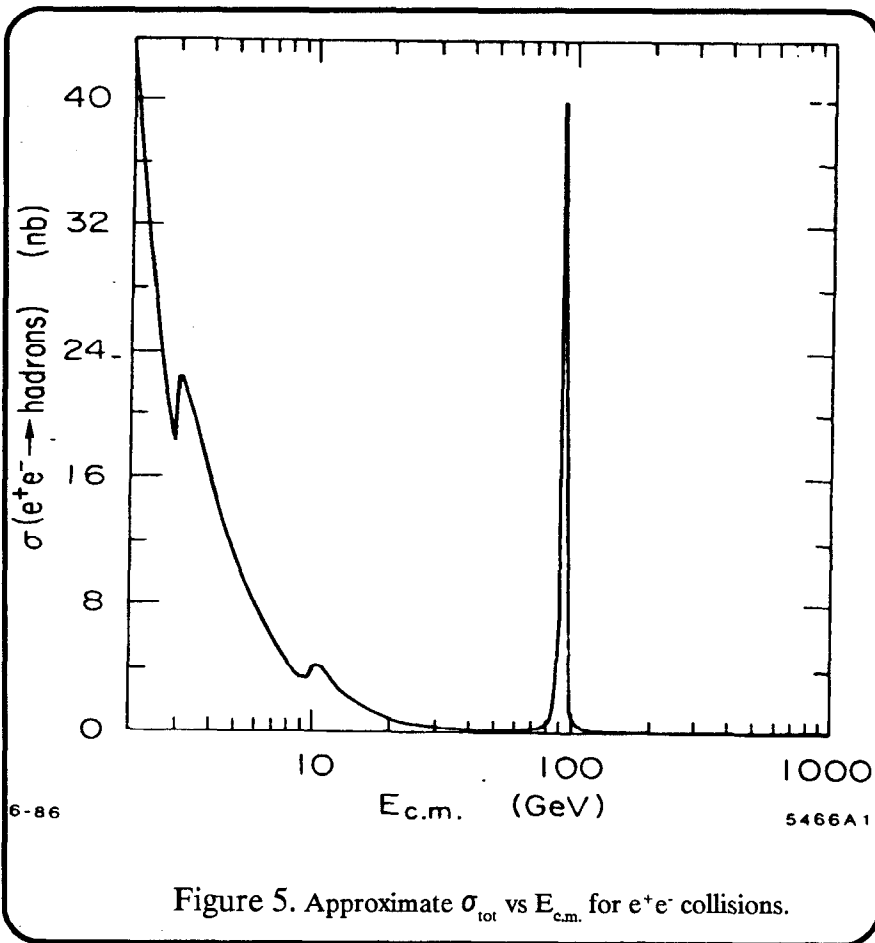


Figure 5. Approximate σ_{tot} vs $E_{\text{c.m.}}$ for e^+e^- collisions.

	CESR (1990s)	SIN [*] (1995 ?)	SBF [#] (1995 ?)	SLC (1990s)	LEP (1990s)	Lin. Coll. (2000 ?)
E_{cm} (GeV)	10 (4S)	10 (4S)	10-26	93 (Z ⁰)	93 (Z ⁰)	10-20
$\sigma(\text{bb})/\sigma_{\text{tot}}$	0.25	0.25	0.1-0.25	0.15	0.15	0.1-0.25
σ_{tot} (nb)	3.9	3.9	0.05-1.0	40	40	1-3.9
\mathcal{L}_{day} (pb ⁻¹)	10	30	180(E_{Max})	0.2 ⁺	0.6	45-450 ⁺
#BB/200days	2x10 ⁶	6x10 ⁶	≥1.6x10 ⁶	2x10 ⁵	6x10 ⁵	10 ⁷
$\gamma\beta c\tau$ (mm) _{Lund}	0.01	0.01	0.01-0.5	2.4	2.4	.25-.5
R _{beam pipe} (cm)	2-6	2-6	2-3.5	1-3	6-8	1-3
$\langle n_{\text{ch}} \rangle_{\text{detector}}$	6	6	6-10	20	20	6-10

* New proposal for a e^+e^- storage ring collider optimized for T(4S).
 # Conceptual design for a major upgrade to PEP, the Stanford Beauty Factory (see sections 3-4 of this report).
 + For linear colliders $\langle L \rangle = L_{\text{peak}}/2$, for storage rings $\langle L \rangle = L_{\text{peak}}/3$.

Table 2. e^+e^- collider parameters

$$\Gamma(B^0[\underline{B}^0](t) \rightarrow f[f]) \propto e^{-\Gamma t} \{ (1 + \cos\Delta mt) \times |\rho_f|^2 [1] + (1 - \cos\Delta mt) \times [1] |\rho_f|^2 \} \\ - [+] (2\sin\Delta mt) \times \text{Im}((p/q)\rho_f) \},$$

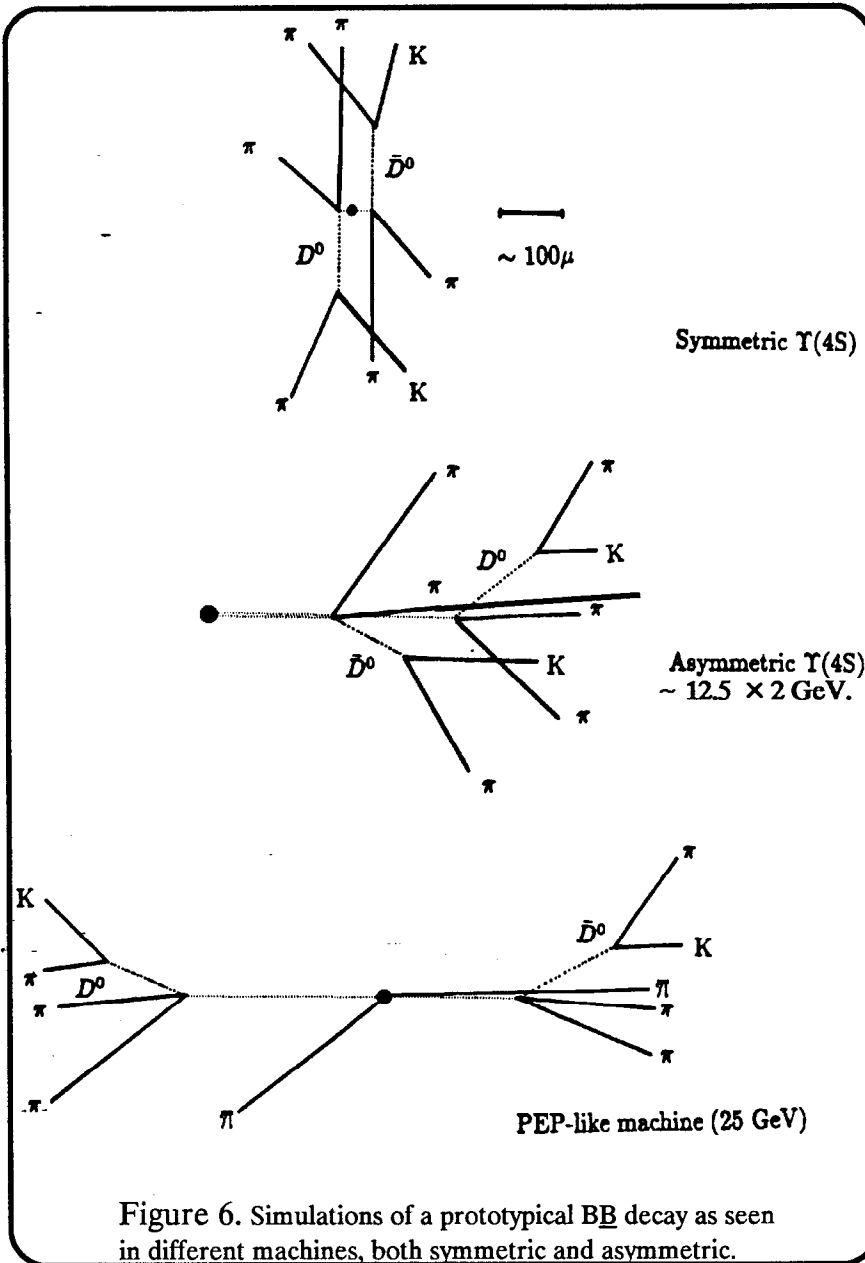


Figure 6. Simulations of a prototypical $B\bar{B}$ decay as seen in different machines, both symmetric and asymmetric.

	CESR (1990s)	SIN (1995?)	SBF (1995?)	SLC (1990s)	LEP (1990s)	Lin. Coll (2000?)
# $B\bar{B}$ /200days	2×10^6	6×10^6	1.6×10^6	2×10^5	6×10^5	10^7
# $C\bar{C}$ /200days	2×10^6	6×10^6	6×10^6	1.6×10^6	5×10^6	4×10^7
# $\tau\bar{\tau}$ /200days	1.7×10^6	5×10^6	4.5×10^6	4.8×10^4	1.5×10^5	3×10^7

Note: $f_s = 0.02$ @ Z^0 , $f_s = 0.21$ in the continuum.

Table 3. Heavy flavor yields from e^+e^- colliders

where, $\rho_f = A(B^0 \rightarrow f)/A(\bar{B}^0 \rightarrow f)$, $p/q = (1 + \epsilon)/(1 - \epsilon)$, and the authors of reference 12 have set $\Delta\Gamma = 0$, and $|p|^2 = |q|^2$ for simplicity, and with the expectation that these approximations are accurate. An example of such a decay is $B^0 \rightarrow \psi K^0$, though the size of the CP violation in each particular case is a matter of some conjecture. (5)

Figure 6 (13) shows examples of events from the decay,

$$B^0 \rightarrow D^0 \pi^+ \pi^- \rightarrow K^+ \pi^- \pi^+ \pi^-$$

and its charge conjugate as seen at different E_{cm} and for the case of, $E_{beam} = 12.2 \text{ GeV}$ on $E_{beam} = 2.0 \text{ GeV}$ with $E_{cm} = 10 \text{ GeV}$, i.e., asymmetric $T(4S)$ production. As the figure qualitatively demonstrates, either symmetric production well into the continuum or asymmetric production at the $T(4S)$ (or other resonances with low Q , e.g., the $T(5S)$ for B^0, \bar{B}^0 production) is needed to enable observation of the spectacular CP violating effects associated with decay length interference.

In addition to enabling the start of the search for CP violation in the B system, some of the machines whose properties are outlined in table 2 have impressive yields of other heavy flavors. The latter is shown in table 3, where large yields of τ 's and charm are shown for the $T(4S)$ and continuum machines. As the branching ratio to $\tau\bar{\tau}$ from the Z^0 is only a few percent, machines presently planned for the Z^0 are not competitive for τ physics.

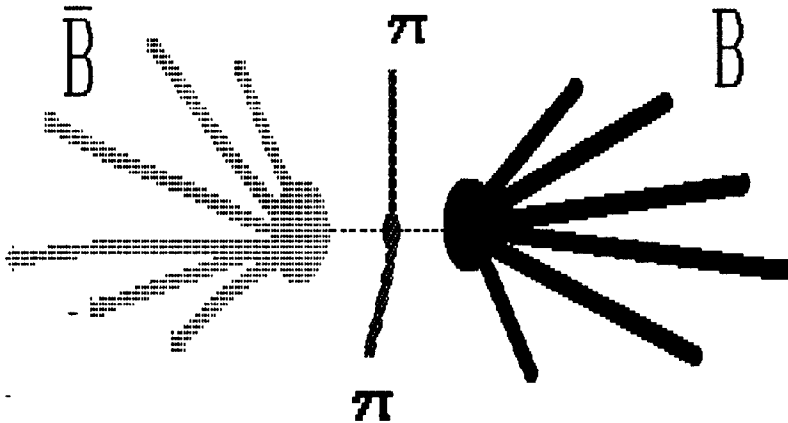


Figure 7. Representation of a $B\bar{B}$ event at $E_{cm} \sim 25$ GeV. The π 's at the e^+e^- vertex come from the central rapidity region and can be removed by a simple rapidity cut. The vertices associated with the B and \bar{B} decays are then revealed.

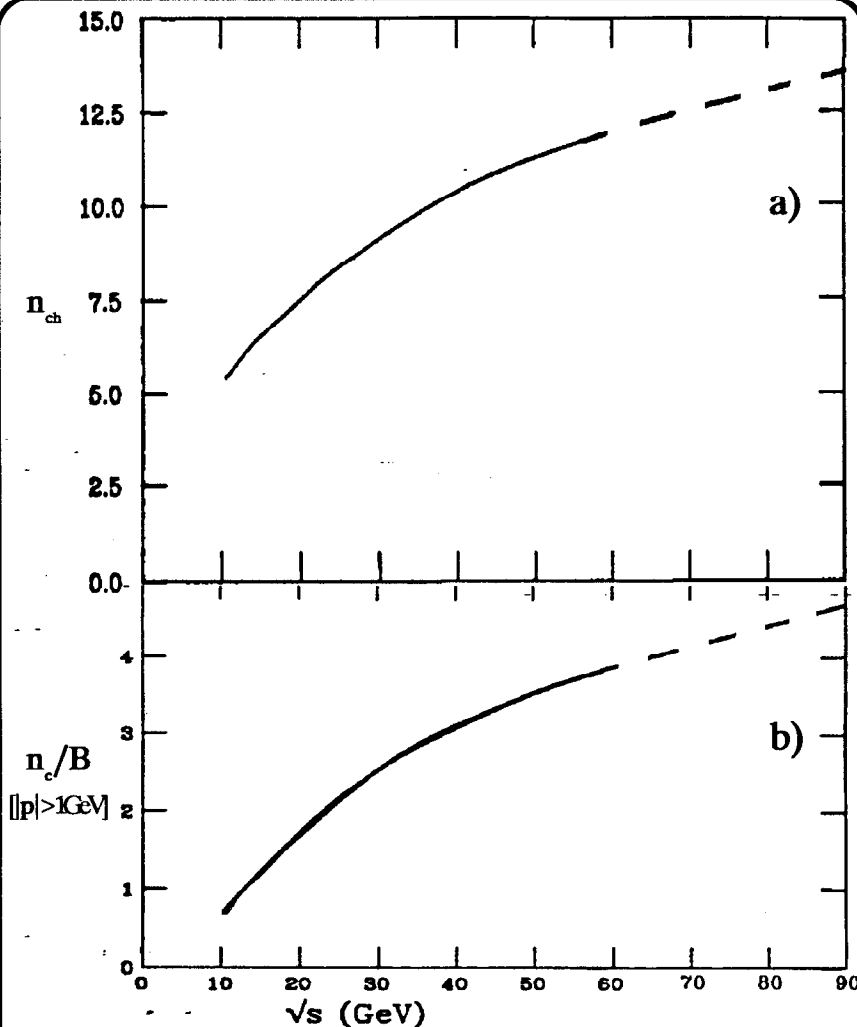
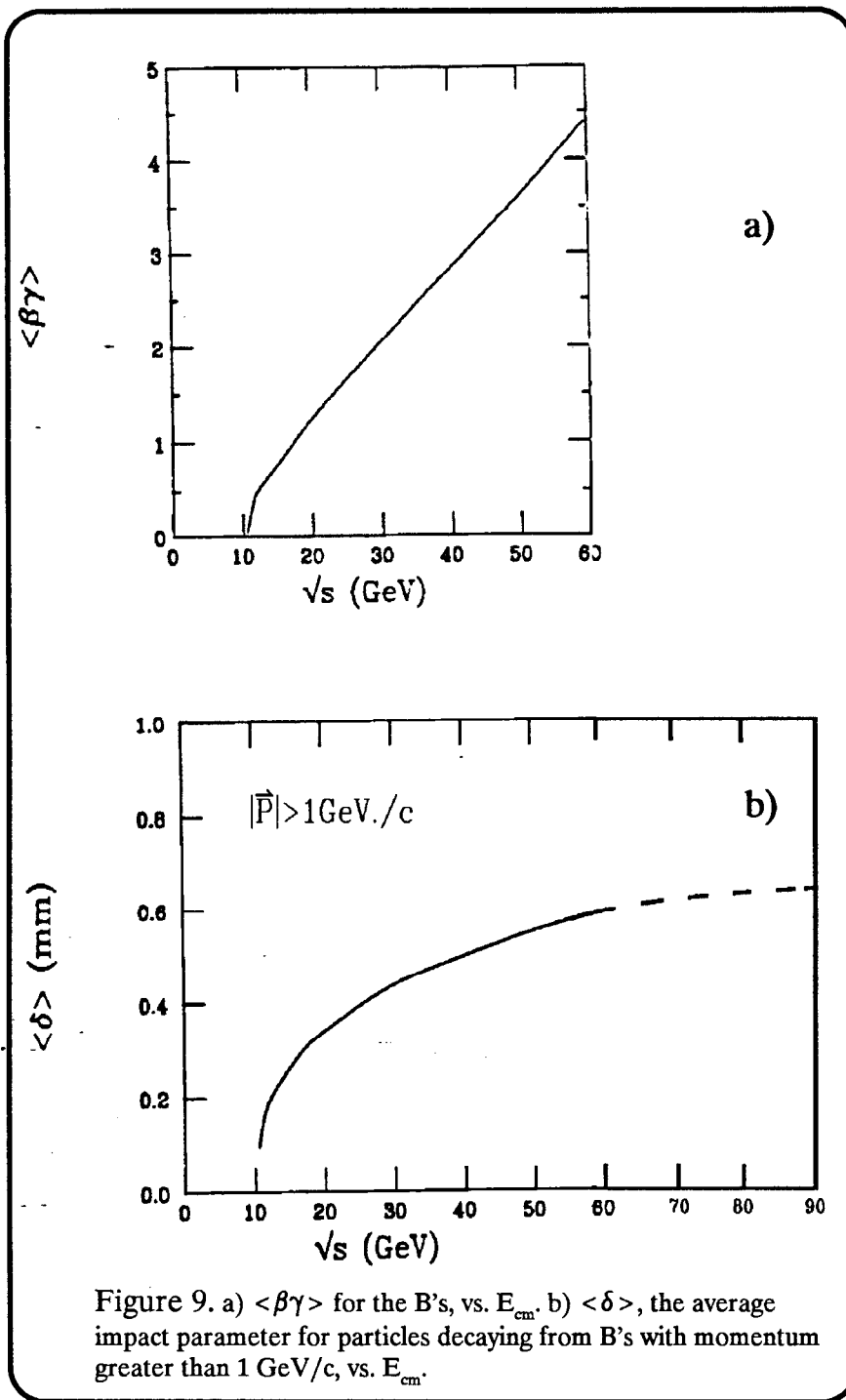


Figure 8. a) n_{ch} , the charged multiplicity in the \bar{B} jet summed with the prompt charged π 's vs E_{cm} . b) n_c/B , the number of charged particles with $|\mathbf{p}| > 1$ GeV/c, vs. E_{cm} . The solid lines are from the Lund M.C., the dashed lines are smooth extrapolations to M_Z .

The efficiency of identification of $B\bar{B}$ pairs and the correct assignment of decay products to the B and \bar{B} are of paramount importance in CP violation experiments. Much of the present deficit in rate at e^+e^- colliders might be made up by clever detection and tagging strategies. The problems at a stationary T(4S) are formidable in this respect; however, it is not so clear at this time whether asymmetric production at lower masses or symmetric production in the continuum optimize efficiencies at significantly different levels. Considerably more work with data and Monte Carlo has to be done for a rational decision to be made. Some work ⁽¹⁴⁾ has been done comparing stationary T(4S) production to that in the continuum, and a summary is shown in figures 7-10.

The Figures were generated using the Lund Monte Carlo ⁽¹⁵⁾ for E_{cm} between the T(4S) and 60 GeV; a smooth extrapolation to the Z^0 at E_{cm} of 92 GeV was then made (shown as dashed lines in some of the figures). Figure 7 defines the general topology of the $B\bar{B}$ events with most of the B jet and \bar{B} jet on opposite sides of the I.P. and a few extra π 's produced at the event vertex. Figure 8a shows n_{ch} , the charged multiplicity in the \bar{B} jet summed with the prompt charged particles, vs E_{cm} . Figure 8b shows $n_c(>1\text{GeV})$, the number of charged particle with momentum > 1 GeV/c, vs E_{cm} . Figure 9 shows $\langle\beta\gamma\rangle$ for the B's and the average impact parameter, $\langle\delta\rangle$, for decay particles with $|\mathbf{p}| > 1\text{GeV}/c$, vs E_{cm} . Though $\langle\beta\gamma\rangle$ grows linearly with E_{cm} , $\langle\delta\rangle$ increases much more slowly for $E_{cm} > 20$ GeV. Note that a "typical" e^+e^- storage ring beam size

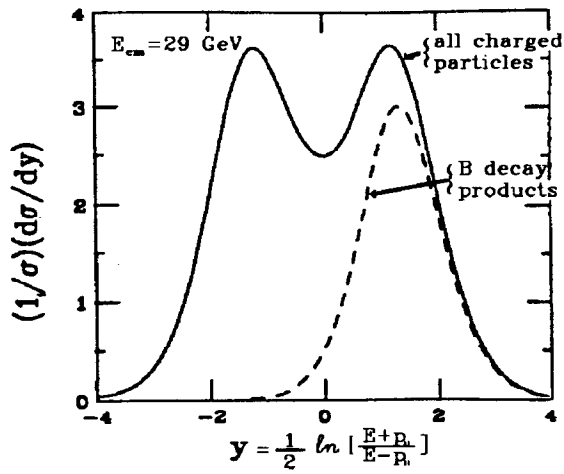


beam size is about $20 \times 350 \mu$ (vertical \times horizontal) with "mini- β ", while the SLC beam size will be $\sim 2 \times 2 \mu$.

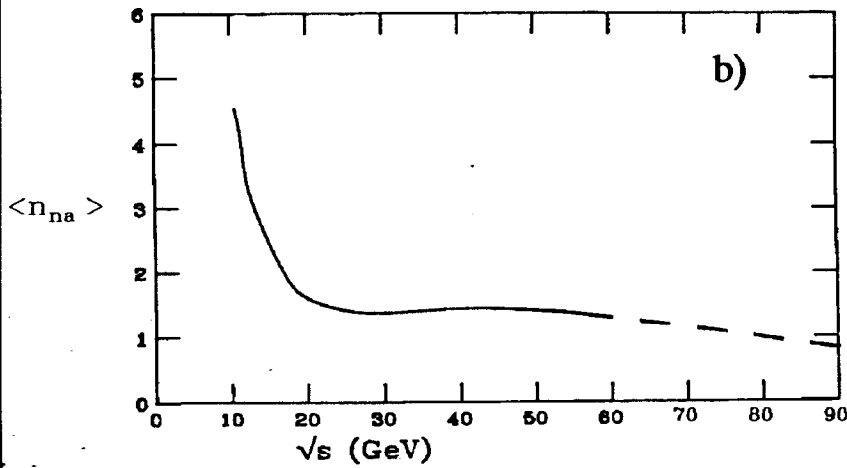
Figures 10 continues with a more quantitative description of the general topology of the $B\bar{B}$ events. Figure 10a shows the distribution in rapidity with respect to the sphericity axis for $B\bar{B}$ events with $E_{cm} = 29$ GeV. The solid line is the distribution for all charged particles, the dashed line for the charged particles from a B decay in each event. Figure 10b shows $\langle n_{na} \rangle$, the mean number of charged particles not associated with the B decay, but within the B decay rapidity region. Figure 10c shows the fraction of tracks with momentum > 1 GeV/c emitted into the hemisphere of the opposite \bar{B} . Clearly, as E_{cm} increases to about 25 GeV a rapid improvement in the isolation of the B and \bar{B} jets occurs with only a mild increase of multiplicity. In addition, $\langle \delta \rangle$ increases dramatically over this range. However, as one proceeds to higher E_{cm} , isolation and $\langle \delta \rangle$ improvement saturate while multiplicity continues to increase. It thus seems that for symmetric colliders, E_{cm} in the range 20 - 30 GeV yield the best topological features for a broad range of B physics which involves B and \bar{B} separation and lifetime determination,

features important to CP violation measurements. As mentioned previously, asymmetric and symmetric collider configurations are still in need of a detailed comparison.

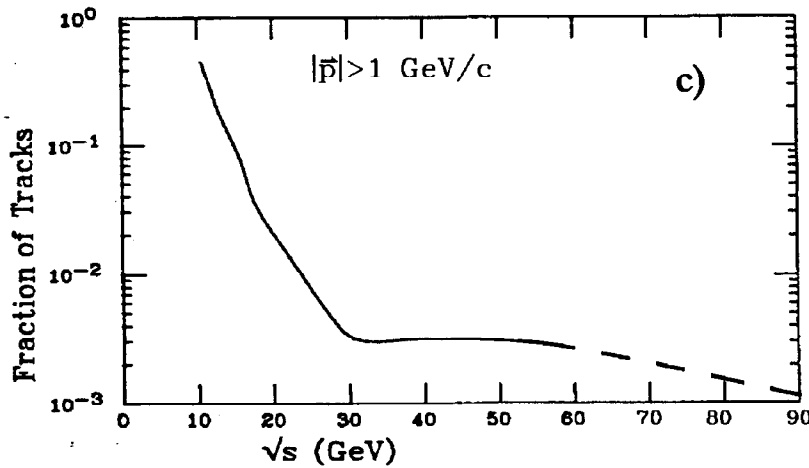
The ability to verticize a $B\bar{B}$ event is a crucial aspect of CP violation measurements. Much work has yet to be done before such capability is available, with the development of 2-D and low mass vertex tracking within 1-2cm of the I.P. essentially a prerequisite. Vertex tracker (VT) resolutions of $\sim 20 \mu$ in both dimensions will be required, as well as material thickness of less than $\sim 0.5\%$ of a radiation length for the VT and beam pipe combination. Note that for the case of a 500 MeV/c particle 0.5%



a)



b)



c)

Figure 10. a) Distribution in rapidity, y , with respect to the sphericity axis for $\underline{B}\bar{\underline{B}}$ events with $E_{cm} = 29$ GeV. The solid line is the distribution for all charged particles, the dashed line for the charged particles from a B decay in each event. b) $\langle n_{na} \rangle$, the mean number of charged particles not associated with the B decay, but in the B decay y region. c) "fraction of tracks" with $|\vec{p}| > 1$ GeV/c emitted into the hemisphere of the opposite \underline{B} .

r.l., at $\theta_z \sim 90^\circ$, the projected error from multiple scattering at the I.P. is $\Delta x \sim 20\mu$. Higher momentum for the particles determining the vertex will be helpful, and so strategies which tag on high energy leptons, as that in reference 16, may be important.

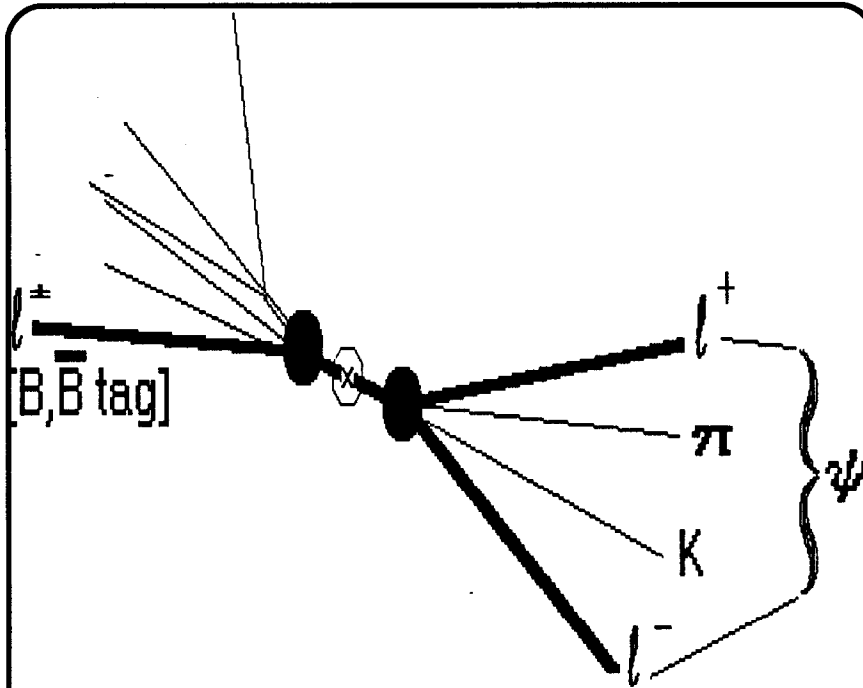


Figure 11. $B\bar{B}$ event with one B vertex tagged by ψ decay to $t\bar{t}$ and the other B identified as B or \bar{B} via a lepton tag. A CP violation measurement is possible using time dependence of difference of decay vertices for B vs \bar{B} .

Figure 11 shows such a $B\bar{B}$ event where one B decays to $\psi(t\bar{t}) + K^*(K\pi)$, and the other B is tagged by a lepton with $E_l > 1$ GeV. (perhaps with a K depending on efficiency). As the B meson inclusive decay to ψ is large, at about 1.25%, the decay of a B to lepton pairs from a ψ is about 0.2%. Given the results of reference 16, and considering a Stanford Beauty Factory (SBF) at design luminosity (see table 1), and a new detector optimized to this type of physics (including VT), one estimates that in a year of data taking (200days): about 6000 $\psi \rightarrow t\bar{t}$ are produced, half of which are detected; about 350 $B_d^0 \rightarrow \psi(t\bar{t})K\pi$ are fully reconstructed; taking $B_s^0/B_d^0 \sim 0.5$, about 150 $B_s^0 \rightarrow \psi(t\bar{t})\phi(KK)$ are fully reconstructed; and finally,

assuming a 0.1% branching ratio, one expects 200 fully reconstructed $B_d^0 \rightarrow \psi(t\bar{t})K_s$ decays. If the opposite $B(\bar{B})$ semi-inclusive tag has a 50% efficiency, a CP violation measurement may be possible using the time dependence of decay for B vs \bar{B} . Given present day speculations on the size of the CP violation in these channels ($\sim 10\% - 50\%$)⁽⁵⁾, about a four year run could be sufficient to see an effect.

3. Machine Design Considerations.

The results of the previous section indicate that a good machine design for the observation of CP violation in B meson decay is a very high luminosity e^+e^- symmetric storage ring operating at $E_{cm} \sim 20-25$ GeV. As SLAC has a machine of the appropriate radius, it is worthwhile to consider some improvements to the present HiLum PEP machine which might possibly achieve the desired level of performance. The two ideas I will discuss involve multiple bunch machines, much like the SIN proposal⁽¹⁷⁾ in-spirit. Indeed, the general design criteria used are very similar to those used by K. Wille in his talk at this workshop, and those used for the SIN proposal⁽¹⁷⁾; this is not an accident.

There are a few basic criteria. The storage ring should have many bunches; the beam should fill the

available physical aperture at all operating energies; there should be only one I.R., or two at the most, where the beams collide; there should be a small β_y at the I.R., β_y^* . These considerations result from the following formula,

$$\mathcal{L} \propto (nf_u) \times \epsilon_{x0} \times (\Delta\nu)^2 / \beta_y^*$$

where, nf_u is the number of bunches, n , times the revolution frequency, f_u , (nf_u is independent of machine size for the same inter-bunch spacing), ϵ_{x0} is the natural horizontal emittance of the beam, and $\Delta\nu$ is the linear tune shift.

Assuming that the single bunch characteristics transfer to the multi-bunch case (no easy feat), the reason for the first factor is evident. More bunches means more luminosity (maybe even linearly with the number of bunches). Multi-bunching has been made to work by the CESR group at Cornell⁽¹⁸⁾. The second factor, ϵ_{x0} , should be made as large as possible with cost being the limiting consideration. The larger ϵ_{x0} , the larger the vacuum pipe, magnet apertures, and other apertures have to be. Also, for

machines where r.f. power is a limitation, larger ϵ_{x0} typically means more power. For machines which will operate at E_b appreciably less than E_b^{\max} , wiggler magnets should be used to fill the available physical aperture at the lower E_b .⁽¹⁹⁾ The question of maximum $\Delta\nu$, the third factor, is related to the number of I.R.'s, and will be discussed below. Finally, the influence of β_y^* is clear.

The question of maximal $\Delta\nu$ is important for achieving high \mathcal{L} . Figure 12 shows accumulated machine data plotted,⁽²⁰⁾ $\Delta\nu/\gamma(\times 10^7)$ vs $1/(n\rho)$, where, $\gamma = E_b/m_e$, and ρ is the machine bending radius. The plot shows data from many machines, and from the old (6 I.R.) PEP with 1 and 3 bunches per beam. These data imply (fitted line) that $\Delta\nu$ increases as the number of collisions per unit time decreases, $\propto (n\rho)^{-1/2}$, all other variables equal. That is, as one increases the damping time between collisions, the attainable $\Delta\nu$ increases. There are those that believe there is also theoretical evidence for this scaling law as well.⁽²¹⁾

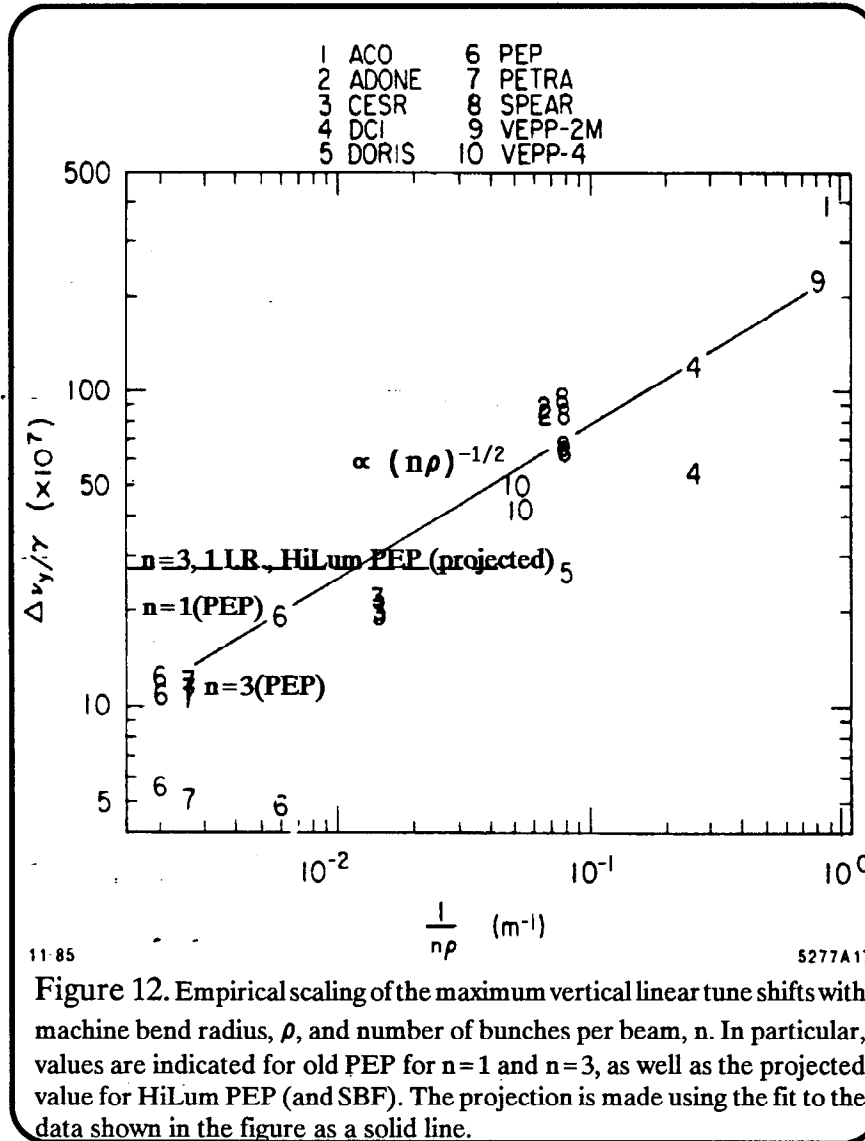


Figure 12. Empirical scaling of the maximum vertical linear tune shifts with machine bend radius, ρ , and number of bunches per beam, n . In particular, values are indicated for old PEP for $n=1$ and $n=3$, as well as the projected value for HiLum PEP (and SBF). The projection is made using the fit to the data shown in the figure as a solid line.

Such a scaling law favors machines with fewer I.R.'s, with one I.R. being optimum. The newly completed HiLum PEP has but one I.R. and will yield an important test of the scaling law with $\Delta\nu \sim 0.08$ expected at $E_b = 14.5$ GeV. This value is shown on the figure as, $n=3$, 1 I.R., HiLum PEP (projected). The scaling law also favors the use of wiggler magnets that do not only fill the aperture of the storage ring, but also excite maximum damping consistent with available r.f. power. The installation of such wigglers at PEP, motivated by their utility for the synchrotron radiation program, has been previously suggested. ⁽²²⁾

The design numbers that appear later in this report have been obtained from the following formulae ⁽¹⁷⁾ which work reasonably well for existing machines.

$$(I_{\text{bunch}})_{\text{max}} = 698.5 f_u E_b \epsilon_{x0} \Delta\nu,$$

and,

$$L_{\text{peak}} = 1.51 \times 10^{32} [n f_u E_b^2 (1 + \kappa^2)^2 \epsilon_{x0} (\Delta\nu)^2 / \beta_y^*],$$

where, E_b is the beam energy, and κ is the horizontal - vertical beam coupling, $\kappa = (\epsilon_y / \epsilon_x)^{1/2} = (\beta_y^* / \beta_x^*)^{1/2}$. Note that in the above formulae $\Delta\nu_x = \Delta\nu_y = \Delta\nu$ is assumed. For many existing machines "optimal" coupling is $\kappa \sim 0.2$. We also assume that ϵ_{x0} "fills the aperture" as a function of E_b ; this was not assumed in reference 17. Filling the machine aperture at $E_b < E_b^{\text{max}}$ can be done with wiggler magnets placed at proper locations in the machine lattice. ⁽¹⁹⁾

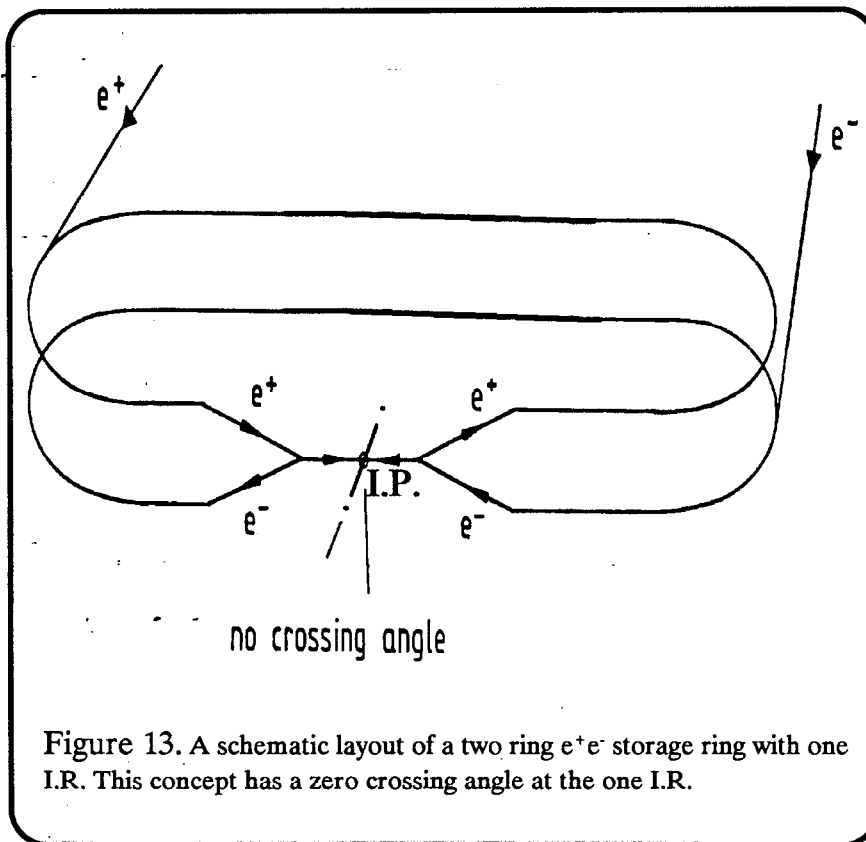


Figure 13. A schematic layout of a two ring e^+e^- storage ring with one I.R. This concept has a zero crossing angle at the one I.R.

Figure 13 shows a schematic layout of a two ring machine with one I.R. Following the design of K. Wille, ⁽¹⁷⁾ a zero crossing angle is taken at the I.P. In order to accomplish a zero crossing geometry a combination of electric or time varying magnetic, and static magnetic guide fields are needed. Static magnetic guide fields alone bend the e^- and e^+ beam in the same direction, as the e^- and e^+ are moving in opposite directions (this is why single ring storage rings work). Figure 14a ⁽²³⁾ shows the geometry needed and illustrates the principle of operation of an r.f. separator. Figure 14b ⁽¹⁷⁾ shows a possible geometry using electrostatic separator plates. As is discussed by Wille, ⁽²³⁾ both techniques need further development with a decision for one scheme or the other based on the results of experiments.

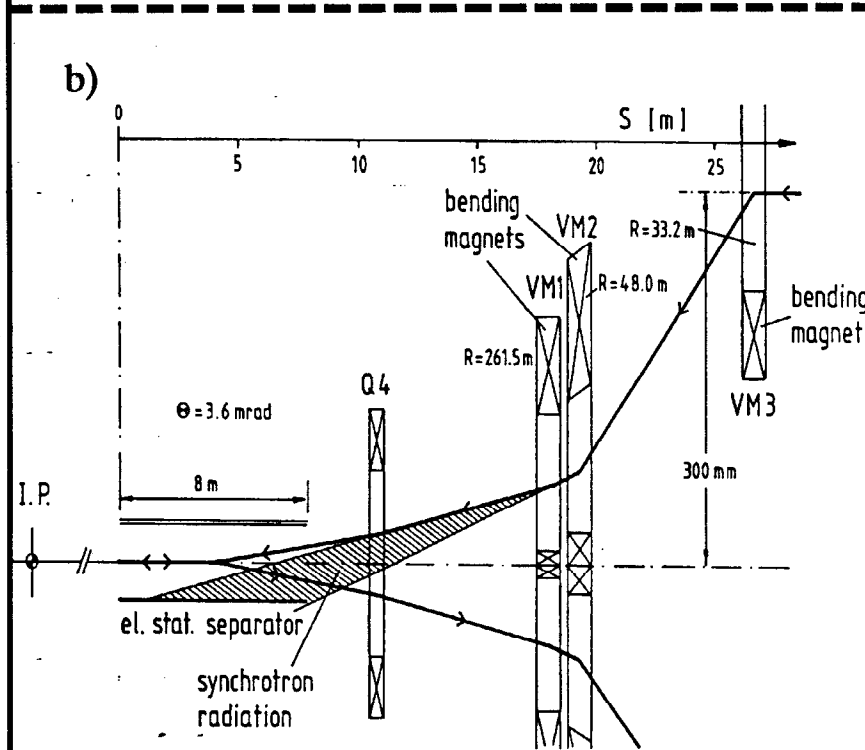
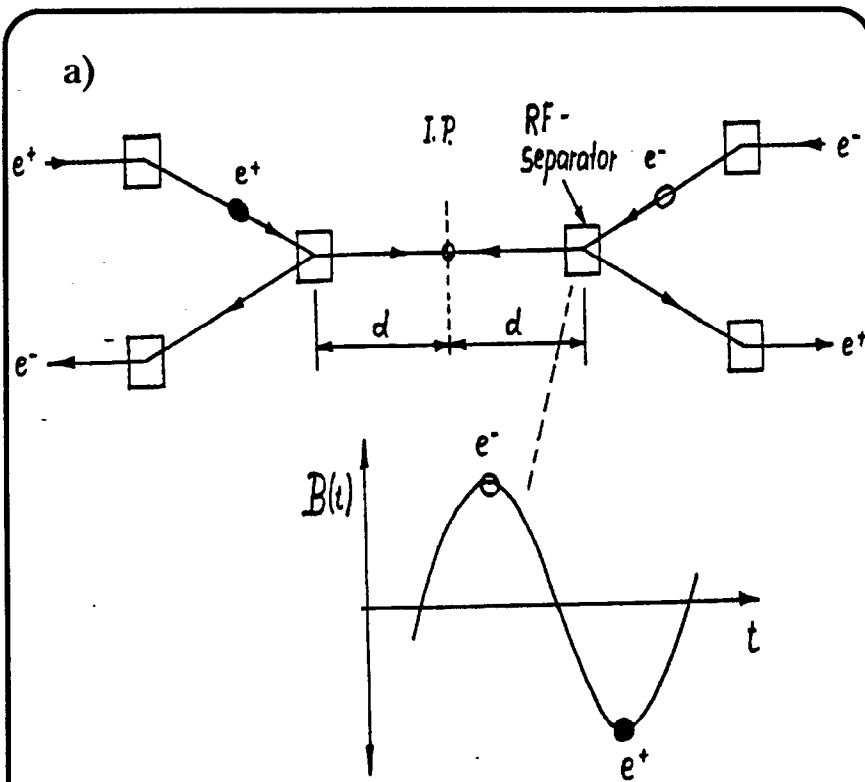
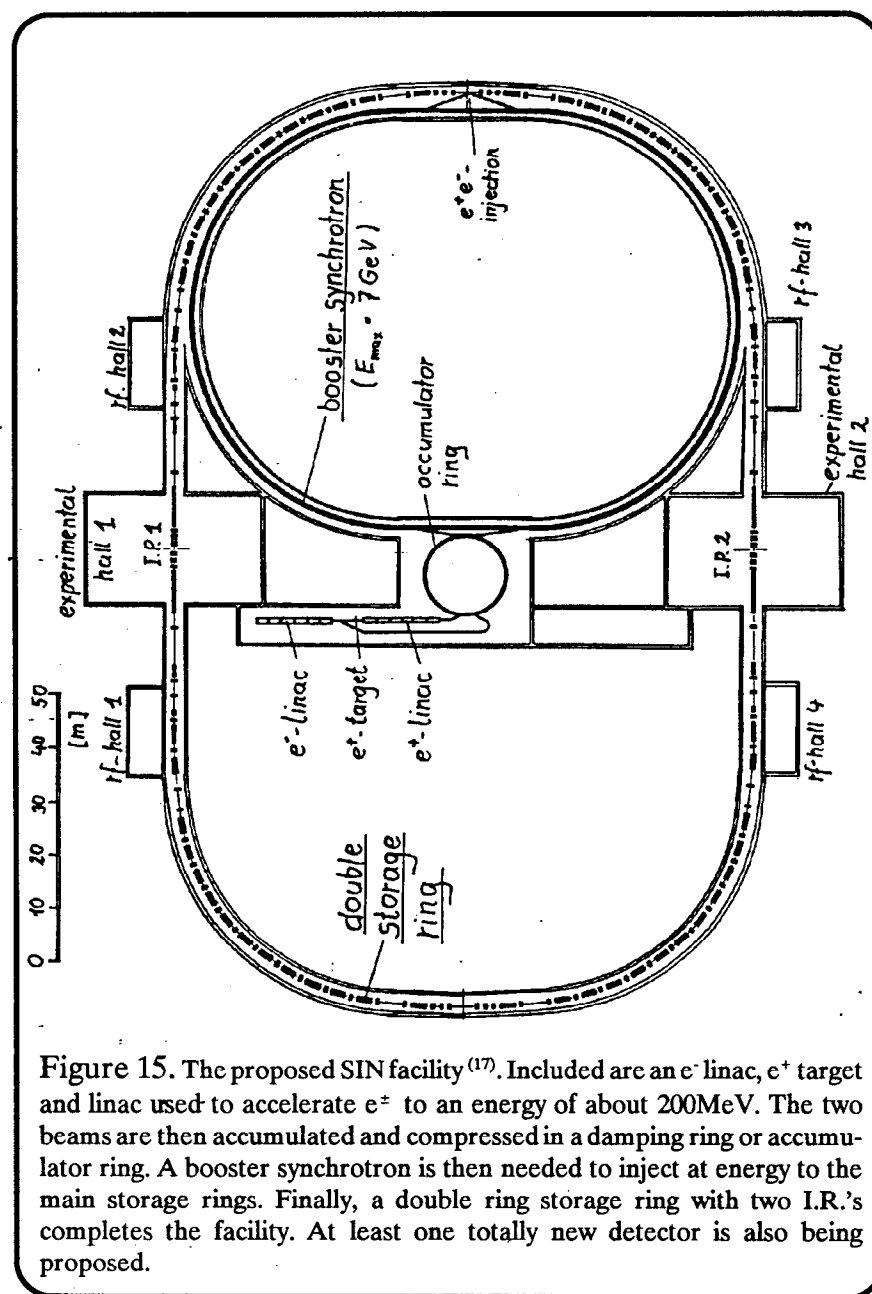


Figure 14. a) Geometry needed for a zero angle crossing I.R. Also shown is the principle of operation of an r.f. magnetic separator. b) A more detailed geometry from the SIN proposal for a zero angle crossing I.R. using electrostatic separator plates.

3b. Scaling from the SIN design to a Stanford Beauty Factory (SBF).

Figure 15 shows a plan view of the proposed SIN B-Meson factory ⁽¹⁷⁾. The facility includes e^+ sources, an accumulator ring, a booster synchrotron allowing injection to a maximum of 7 GeV., a double ring storage ring which is 520 m in circumference, and two experimental halls enclosing 2 I.R.s. This machine will be a symmetric collider intended for optimum operation at the T(4S). It will be a multiple bunch machine, ultimately operating with 12 bunches per beam (inter-bunch spacing of 43 m), with currents up to 0.75 A per beam.

In order to scale this design to $E_{cm} \sim 25$ GeV, we will consider the major points mentioned in section 3a:



First, the number of bunches. A minimum bunch spacing of 20 - 40 m is dictated by the rise time of the feedback systems needed to control the multi-bunch instabilities, and the geometry of the I.R. The collisions should be head-on to avoid the problems that DORIS I had. The long straight sections of HiLum PEP are particularly amenable to a double ring upgrade as there is considerable room for matching the arcs to the I.R.'s. With a separation of 31m, 70 bunches can be put uniformly in a double ring machine. In addition, the very long straight sections of 117 m, see figure 16, allow an initial phase of multi-bunching to be done without a double ring (SBF₀). For separation in the straight sections only (there is not enough aperture in the arcs) the present PEP ring can be used. This scheme allows 15 bunches per beam placed in three groups of 5 bunches with each bunch in a group separated by 20 m from the next. The single ring multi-bunch PEP, SBF₀, has about 5 times fewer bunches and thus five times lower L than a double ring; however, this scheme is relatively inexpensive to build, and could yield a factor of five in L over the present HiLum PEP.

Figure 15. The proposed SIN facility ⁽¹⁷⁾. Included are an e^- linac, e^+ target and linac used to accelerate e^+ to an energy of about 200MeV. The two beams are then accumulated and compressed in a damping ring or accumulator ring. A booster synchrotron is then needed to inject at energy to the main storage rings. Finally, a double ring storage ring with two I.R.'s completes the facility. At least one totally new detector is also being proposed.

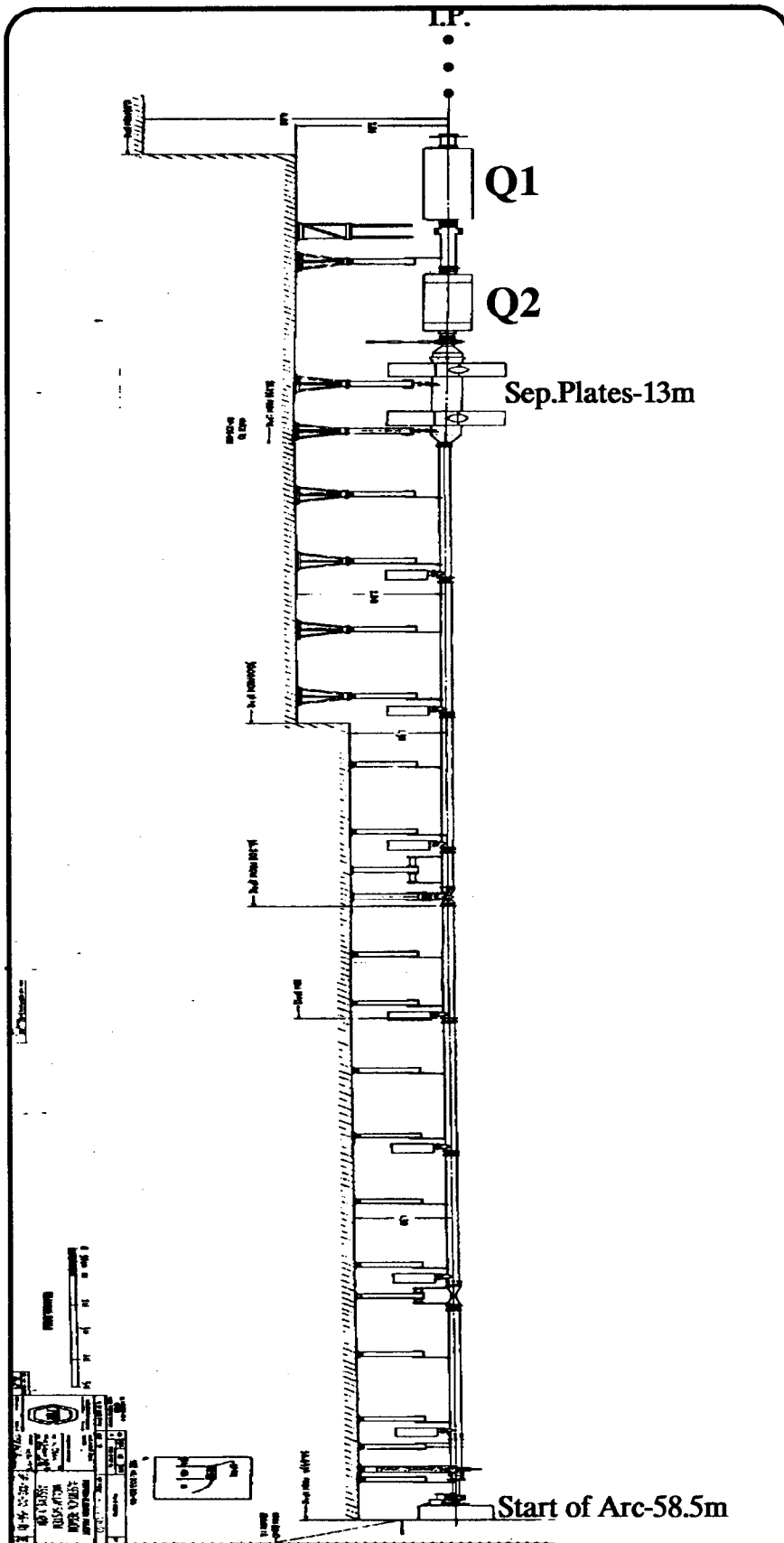


Figure 16. A PEP straight section shown from Q1, the first quad after the I.P., to the start of the bending arcs at 58.5m from the I.P. This section corresponds to all I.R.'s but I.R. 2 which has an additional quad, Q2.5.

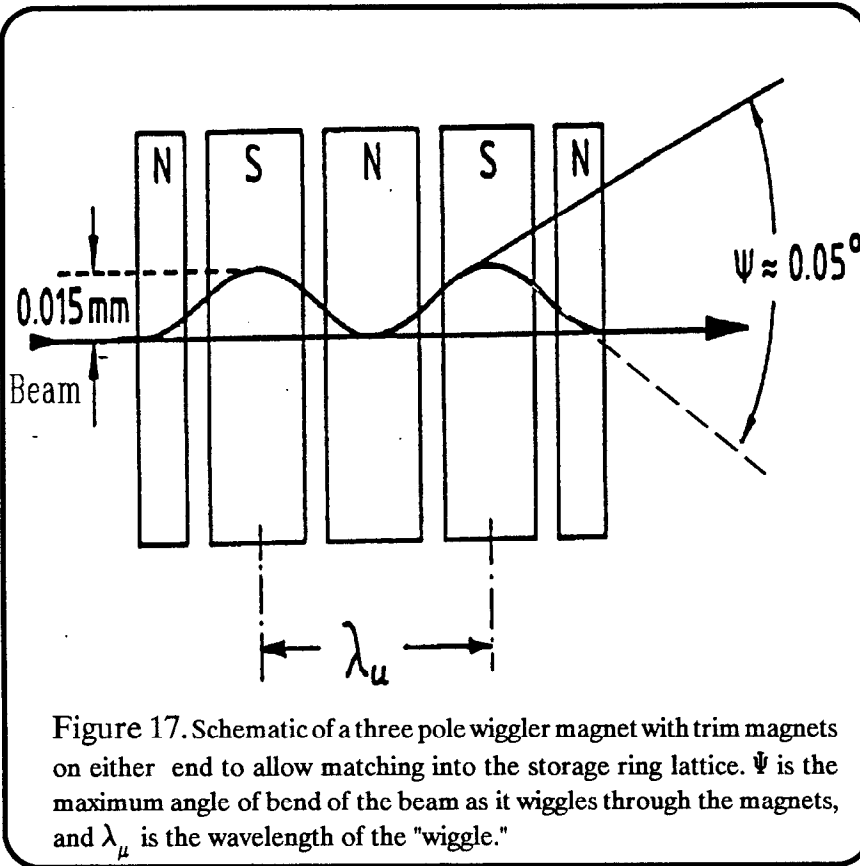


Figure 17. Schematic of a three pole wiggler magnet with trim magnets on either end to allow matching into the storage ring lattice. Ψ is the maximum angle of bend of the beam as it wiggles through the magnets, and λ_u is the wavelength of the "wiggle."

Second, the aperture. The SIN machine ⁽¹⁷⁾ is planned to have quite a large emittance allowing $\epsilon_{x0} = 8.3 \times 10^{-7}$ m-rad. This is accomplished by keeping $\beta \leq 30$ m in the ring, rather than by having a larger than normal physical aperture. For the SBF calculations we will use the present HiLum PEP emittance, $\epsilon_{x0} = 1.2 \times 10^{-7}$ m-rad. Note that ϵ_{x0} is defined by $\sigma_x \approx \sqrt{(\epsilon_{x0} \beta_x)}$, ($\eta = 0$). Wigglers are needed to bring beam size to the aperture limit at $E_b < 14.5$ GeV, and to assure the tune shift limit of the design. Figure 17 shows a schematic of a three pole wiggler with trim sections at either end which allow a match into the machine lattice.

The use of wiggler magnets has been extensively discussed in references

19 and 22. I will review the basic principles of operation below. The increase in emittance, $\epsilon_{x0}^w / \epsilon_{x0}$, is given by,

$$\epsilon_{x0}^w / \epsilon_{x0} \approx [1 + (\langle H_w \rangle L_w / (\langle H_0 \rangle L_0)) \times (\rho_0 / \rho_w)^3] / [1 + (\rho_0 / \rho_w)^2],$$

where, ρ_0 is the main bend radius of the storage ring, ρ_w is the wiggler magnet bend radius, L_0 is the length of the machine bends, and L_w is the effective length of the wiggler. The H's are more complicated, with H_0 being a complex function of the machine lattice. ⁽²⁴⁾ H_w is reasonably approximated by,

$$\langle H_w \rangle \sim \langle \eta^2 / \beta \rangle_w,$$

where the average is taken over the length of the wigglers. Note that for the old PEP, $\langle H_w \rangle / \langle H_0 \rangle \sim 1$.

The stored beam's damping time is given by,

$$\tau_w / \tau_0 \sim [1 + (L_w / L_0) \times (\rho_0 / \rho_w)^2]^{-1},$$

where, τ_0 is the damping time of the beam without wigglers. In order to damp the beam more quickly r.f. power is needed. The energy loss per turn, U_0 , increases as wiggler strength is increased, and,

$$U_{0w}/U_0 = \tau_0/\tau_w.$$

The above formulae show that by adjusting η and β at the wiggler location, one can tune the trade off between beams size and damping time over a wide range, however, at a cost of additional r.f. power.

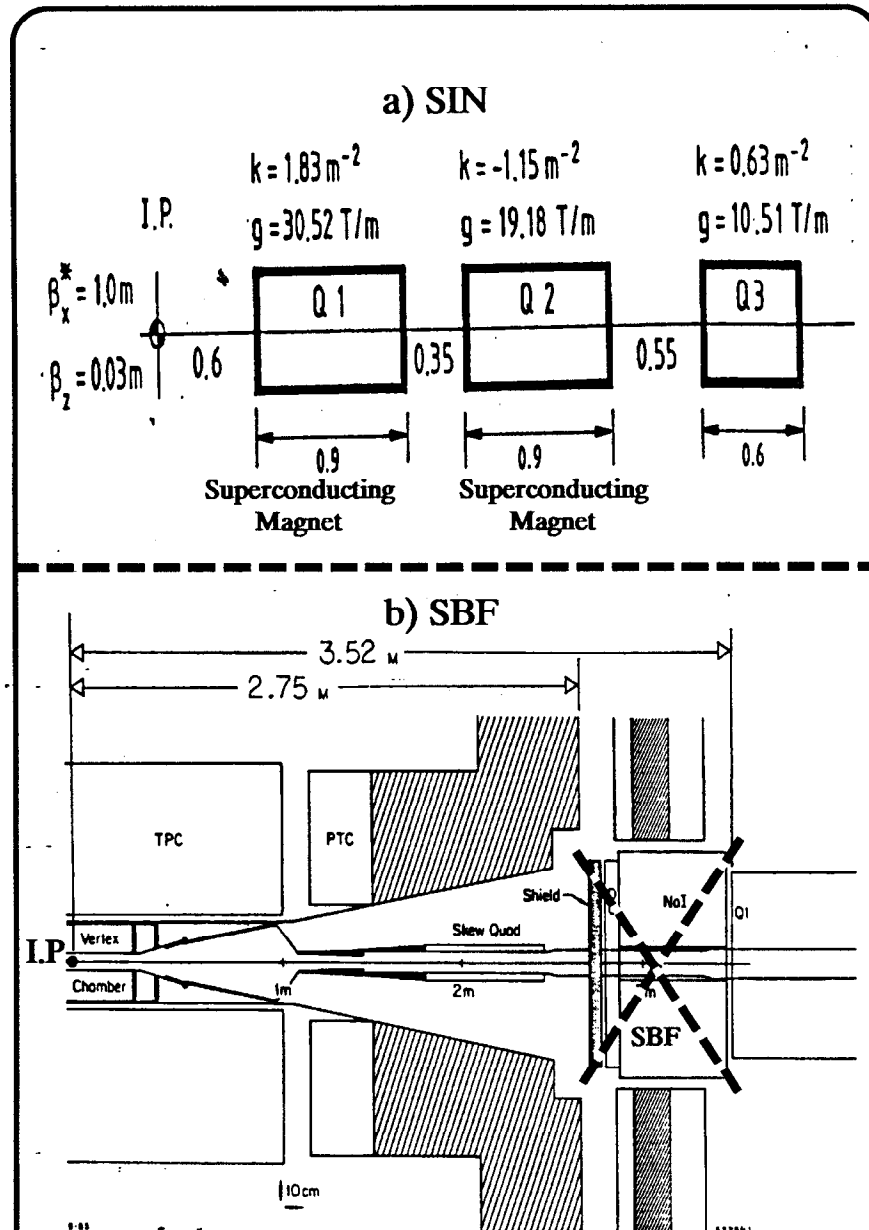


Figure 18. a) Preliminary design of the SIN I.R.⁽¹⁷⁾ This design requires two (pairs) of superconducting quads with the face of the nearest quad at 0.6m from the I.P. b) Concept for the SBF I.R. The first large quad is a standard PEP Q1 at a distance of 2.75m from the I.P. This should allow for $\beta_y^* \sim 3\text{cm}$ as is the case for SIN. The present TPC/ 2γ forward detector will have to be redesigned to accommodate the new Q1 location.

Third, the tune maximum tune shift. As DORIS II has achieved $\Delta\nu_{\max} \sim 0.025$, Wille⁽²³⁾ has been conservative in his design specs. in specifying $\Delta\nu_{\max} \sim 0.025$ as the initially achievable tune shift for the proposed SIN machine. This machine will be operating in the same energy regime, and has other features reminiscent of DORIS II. However, Wille projects that $\Delta\nu_{\max} \sim 0.05$ will be possible eventually. PEP has achieved $\Delta\nu_{\max} \sim 0.05$ in its old incarnation and the scaling laws discussed in section 3a imply that $\Delta\nu_{\max} \sim 0.08$ will be possible for the SBF (and SBF₀).

Fourth, the β_y^* . Figure 18a shows the low beta insertion for the proposed SIN machine. This design is state of the art with two superconducting quads required (per side), and only 0.6m between the face of the last superconducting quad and the I.P. β_y^* is quite modest at 3cm and can't be made much smaller as dictated by the natural bunch length for storage rings with r.f. frequency in the 350 - 500M MHz range; β_y^* should be no smaller than $\sim 1.5 \times \sigma_z^{\text{beam}}$. Figure 18b shows a possible I.R. arrangement for the SBF (and SBF₀). With the first major quads at 2.75 m, a 3 cm β_y^* is possible. In addition, a very smooth beam pipe, and minimal length of r.f. cavities are needed in all machines of this type due to the

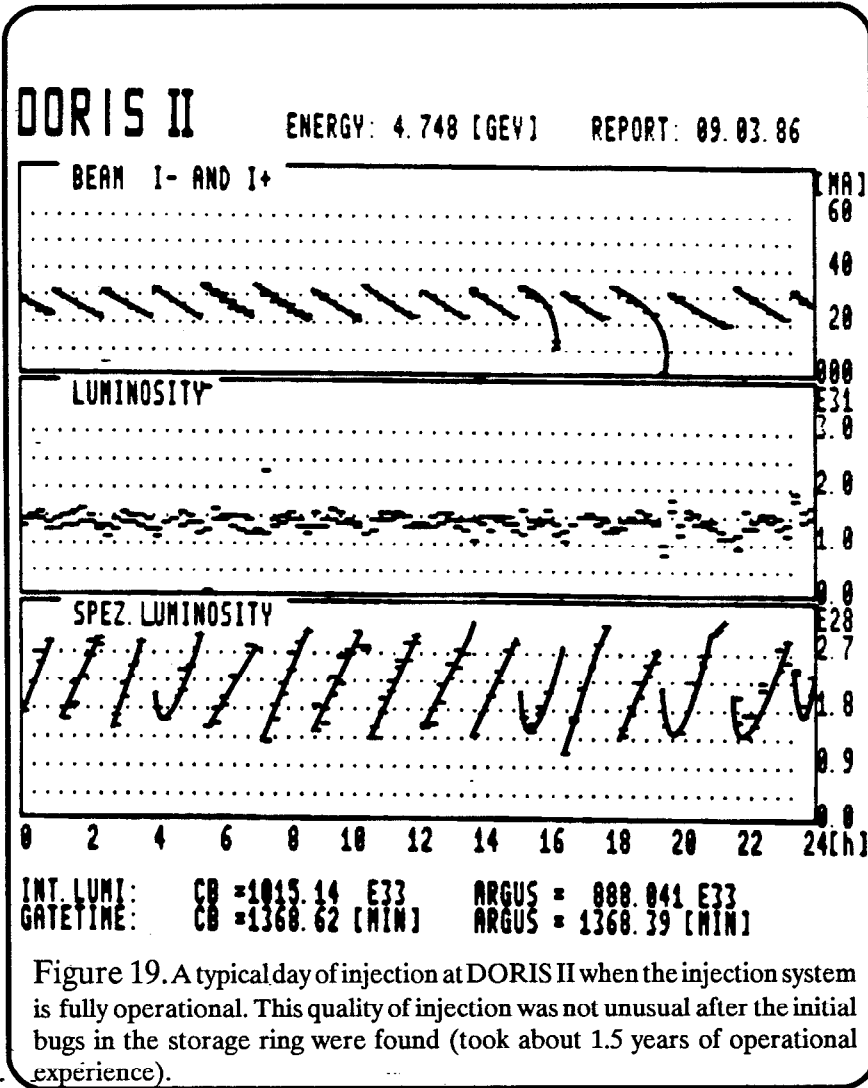


Figure 19. A typical day of injection at DORIS II when the injection system is fully operational. This quality of injection was not unusual after the initial bugs in the storage ring were found (took about 1.5 years of operational experience).

high currents and the possible effects of beam bunch lengthening.

Finally, superior injection is required so as to allow rapid filling of the storage ring. The stored current goals for the SIN proposal are, $I_{max} \sim 0.75$ A per beam, while for the full blown SBF concept $I_{max} \sim 0.85$ A per beam. In the case of the SBF, injection at 5×10^9 particles per pulse, at a 60 Hz injection rate, and with 50% capture efficiency will take ~ 4 min per beam. As the proposed SIN ring has a circumference which is about 4 times smaller, it would require about 1 min per beam with the same filling rate. For topping off (both machines will fill at energy without the need for ramping), divide the times by ~ 2 . The SBF₀ would need about 5 times less time than the SBF, or about the same as the SIN proposal. DORIS II has actually achieved impressive filling rates, with topping off typically requiring only one or two minutes.

Figure 19 shows a typical days record when the system is fully operational. However, the three new machines discussed here have injection requirements which are an order of magnitude or more greater than DORIS II. Powerful injectors are required or much longer times will be taken for fills.

4. Luminosity Estimates

Figure 20 shows the design luminosity for the SIN proposal. Wille expects the Luminosity to increase in stages ⁽²³⁾ as more is learned and improvements are made. The bottom curve in the figure is expected within the first year of operation, with subsequently higher levels achieve as operating experience is gained. Finally, after some years of operation, $L_{peak} \sim 3 \times 10^{33} \text{ cm}^{-2}\text{sec}^{-1}$, is projected at the T(4S).

The SBF can also be staged. Initially, the SBF₀ can be built, at modest cost, and operational experience with multi-bunch and high currents will be gained. If and when it appears possible and desirable to gain an additional factor of 5 in luminosity the SBF is a candidate design. Table 4 gives some parameters

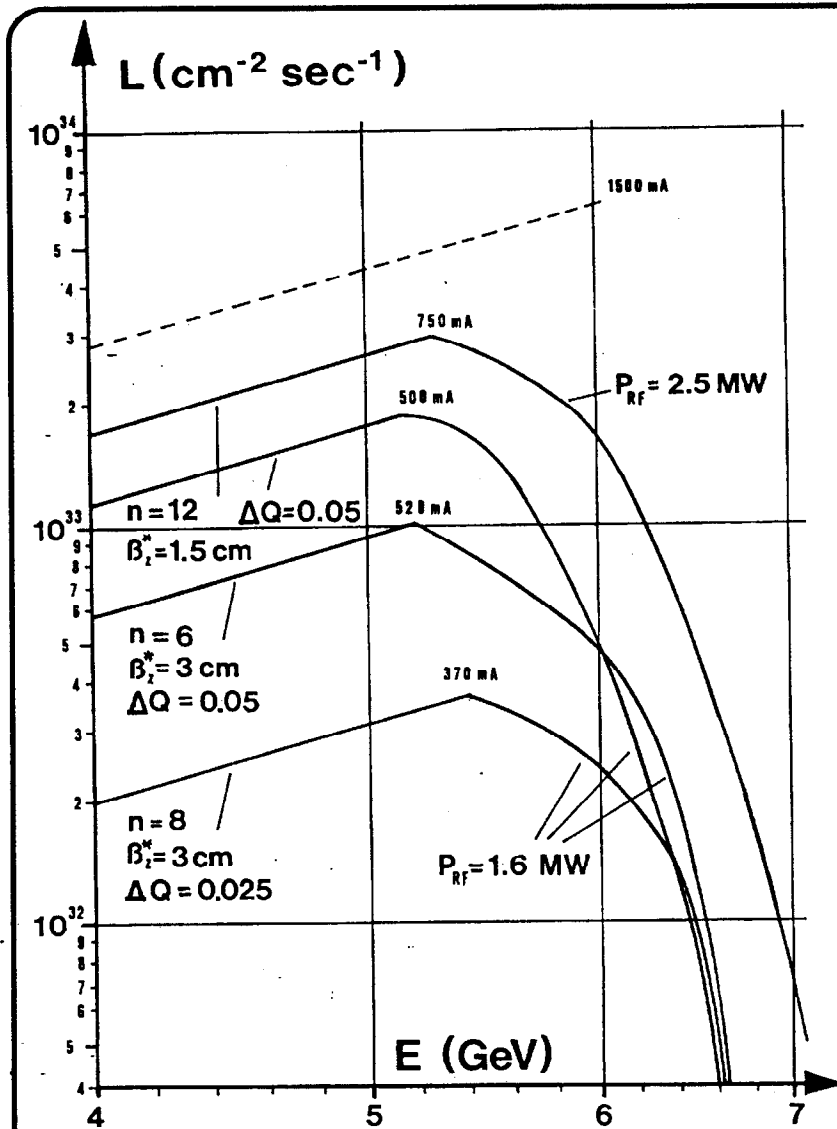


Figure 20. The design luminosity for the proposed SIN machine. Improvement of \mathcal{L} is expected in stages as more is learned and machine improvements are made. The bottom curve is expected within the first year of operation, with subsequently higher levels achieved as operating experience is gained. Finally, with $n=12$, $\Delta\nu = 0.05$ ($\Delta Q \equiv \Delta\nu$), β_z^* ($\equiv \beta_z^*$) = 1.5 cm, and $I_{\text{beam}} = 0.75\text{A}$, $\mathcal{L}_{\text{peak}} \sim 3 \times 10^{33} \text{cm}^{-2}\text{sec}^{-1}$ is projected.

lifetime, and so a crucial window on CP violation is lost. The SBF concept may be sufficient to achieve a measurement of CP violation in the B system, but the development of such a machine and the measurements will probably require a staged effort over a decade. In addition, if an e^+e^- machine, a B-factory will yield more than 10^7 τ and C decays while the B's are being produced. Thus many questions involving heavy flavor physics can be addressed at such a facility.

It is clear that much development work is needed in both the machine physics and detector design to achieve the CP violation measurement goals. It seems prudent to start in earnest soon, and to expect an extended effort.

of the SBF₀ and SBF. At $E_b = 12.5$ GeV, $\mathcal{L}_{\text{peak}} \sim 10^{33}$ is projected for the SBF₀, and $\mathcal{L}_{\text{peak}} \sim 6 \times 10^{33}$ for the SBF. The large r.f. power required for the SBF and perhaps the SBF₀ as well, may demand the use of LEP type klystrons and superconducting cavities. The klystrons are now "off the shelf" items obtained from Philips (Cat. #YK1350), are rated for 1MW output power, and have a central frequency of 352.21 MHz, the PEP r.f. frequency. Figure 21 shows a schematic of the Philips tube. In addition, superconducting cavities at the same frequency should also be available from European industrial sources in a couple of years (as a small add on order to LEP's).

5. Conclusions

The chance to gain insight into a possible new mass scale plus many other physics opportunities that a sample of 10^7 B decays rings is a physics justification for a B-factory by itself. The machines discussed in section 3 of this paper all can produce $\sim \text{few} \times 10^6$ B decays in a reasonable running time; however, the SIN design (and CESR as well) which optimizes the machine for symmetric beams with E_{cm} at the T(4S) does not allow for measurements of B

6. Acknowledgements

Many of my colleagues have contributed to the content of this report. There are three major areas that I would like to separately acknowledge. First, my motivation to pursue this nascent field of CP violation in the B system was sparked by extensive conversations with I. Bigi (SLAC), A. Fridman (CERN/SLAC/UCLA), F. Gilman (SLAC), H. Harari (Weizmann/SLAC), P. Oddone (LBL). These colleagues have also suggested examples to clarify the physics goals, a number of which I have used in this report. Second, the section on "where to B" was packed with the work of W. Hofmann (Berkeley) and G. Wormser (SLAC). Finally, the genesis of the SBF machine concepts have been strongly influenced through many discussions with M. Donald and D. Ritson of SLAC, in addition important contributions to these ideas have been made by many members of the SLAC accelerator physics group, and, H. Nesemann (DESY), D. Rubin (Cornell), R. Siemann (Cornell), R. Talman (Cornell), K. Wille (Dortmund), H. Wiedemann (SSRL).

	HiLum PEP	SBF ₀	SBF
circumference(m)	2200	2200	2200
#rings	1	1	2
#I.R.'S	1	1	1
n	3	15	70
β_y^*	4	3	3
$\Delta\nu$	0.08	0.08	0.08
Wigglers	no	yes	yes
$L_{peak} (\times 10^{32} \text{cm}^{-2} \text{sec}^{-1})$ @12.5 GeV/beam @5.3 GeV T(4S)	1.4 NA	13.2 2.4	61.6 11.1
$\langle L \rangle (\text{pb}^{-1}/\text{day})$ @12.5 GeV/beam @5.3 GeV T(4S)	4.0 NA	38.0 6.8	177.3 31.9
$P_{beam} (\text{MW})$ @12.5 GeV @5.3 GeV T(4S)	0.3 NA	4.0 0.7	18.8 3.4
$I_{bunch} (\text{ma})$ @12.5 GeV @5.3 GeV T(4S)	8.3 NA	11.9 5.1	11.9 5.1
$I_{beam} (\text{ma})$ @12.5 GeV @5.3 GeV T(4S)	24.9 NA	178.9 75.9	834.9 354.0
BB pairs/200days($\times 10^6$) @12.5 GeV @5.3 GeV T(4S)	0.04 NA	0.35 1.4	1.6 6.4

Table 4. Parameters for e^+e^- storage rings based on improvements to PEP. The present HiLum PEP is compared to the SBF₀ and SBF. The parameters discussed in the text are used to calculate projected performance.

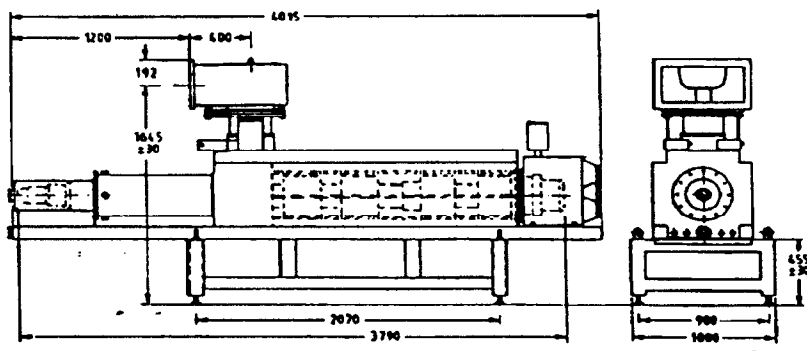


Figure 20. Philips YK 1350 continuous-wave high-power klystron. Water cooled, high efficiency, fixed frequency (353.31MHz), 1Mw klystron in metal-ceramic construction. Cost per klystron is ~ \$1m installed. Dimensions in the figure are in cm.

References

1. H. Albrecht, et.al. (ARGUS), Phys. Lett. 192B, 247(1987).
2. For example see: I.I. Bigi and A. Soni, Phys. Rev. Lett. 53, 1407(1984); I.I. Bigi and A.I. Sanda, Phys. Rev. D29, 1393(1984).
3. J.S. Hagelen, Phys. Rev. D20, 2893(1979).
4. For a recent review see the talks of: A. Montag, D. Muller, and R. Ong, Proceedings of the 2nd International Symposium on the Production and Decay of Heavy Flavors, Stanford University, Stanford, CA, Sept 1-5, 1987, proceedings edited by E.D. Bloom and A. Fridman, (1988).
5. I.I. Bigi and A.I. Sanda, SLAC-PUB-4299, (1987).
6. I. Wingerter (UA-1), Proceedings of the 2nd International Symposium on the Production and Decay of Heavy Flavors, Stanford University, Stanford, CA, Sept 1-5, 1987, proceedings edited by E.D. Bloom and A. Fridman, (1988).
7. B. Winstein, Proceedings of the Fourteenth SLAC Summer Institute on Particle Physics, SLAC Report No. 312, 33(1987).
8. H. Harari, Proceedings of the Twelfth SLAC Summer School on Particle Physics, SLAC Report No. 281, 264(1985).
9. R.N. Mohapatra and G. Senjanovic, Phys. Rev. Lett. 44, 912(1980); Phys. Rev. D23, 165(1(81). See also, H. Harari, Proceedings of the Fourteenth SLAC Summer School on Particle Physics, SLAC Report No. 312, 1(1987).
10. Much effort has gone into these questions at past conferences and workshops. Below is a partial list:
 - Workshop on e^+e^- Physics at High Luminosities, SLAC Report No. 283, proceedings edited by H. Paar, (1985);
 - 1st International Symposium on the Production and Decay of Heavy Flavors, University of Heidelberg, Heidelberg, FRG, May 20-23, 1986, proceedings edited by K.R. Schubert and R. Waldi, DESY report (1986);
 - Critical Issues in the Development of New Linear Colliders, University of Wisconsin, Madison, WI, August 27-29, 1986;
 - The Linear-Collider BB Factory Conceptual Design Workshop, University of California, Los Angeles, CA, Jan 26-30, 1987;
 - 2nd International Symposium on the Production and Decay of Heavy Flavors, Stanford University, Stanford, CA, Sept 1-5, 1987, proceedings edited by E.D. Bloom and A. Fridman, (1988).

11. B. Cox, Invited talk at this workshop.
12. I.I. Bigi and A. I. Sanda, Nucl. Phys. 281, 41(1987); also, ref. 5.
13. Figure 6 is essentially from the talk of P. Oddone presented at the Linear Collider BB Factory Conceptual Design Workshop, University of California, Los Angeles, CA, Jan. 26-30, 1987, proceedings to be published. Oddone discussed both symmetric and asymmetric colliders and their interaction with potential detectors.
14. W. Hofmann, et al, Workshop on e^+e^- Physics at High Luminosities, proceedings edited by H. Paar, SLAC Report No. 283, 35(1985).
15. T. Sjostrand, Comm. Phys. Comm. 27, 243(1982); 28, 229(1983). This relatively early version of the Lund Monte Carlo was tuned by W. Hofmann to match the available data for heavy quark processes.
16. G. Wormser, MarkII/SLC - Physics Working Group Note #9-15, (1987).
17. E. Eichler, et.al., Motivation and Design Study for a B-Meson Factory with High Luminosity, SIN-PR-86-13, (1986).
18. K. Berkelman, talk at this workshop.
19. J.M. Paterson, et. al., PEP note 125, (1975).
20. J. T. Seeman, SLAC-PUB-3825, (1985).
21. R. H. Siemann and R. Talman, Private Communication.
22. H. Wiedemann, Proceedings of the Workshop on PEP as a Synchrotron Radiation Source, held at SLAC, Stanford University, October 20-21, 1987, SSRL Report (1988).
23. K. Wille, Talk at this workshop, and Proceedings of the 2nd International Symposium on the Production and Decay of Heavy Flavors, Stanford University, Stanford, CA, Sept 1-5, 1987, proceedings edited by E.D. Bloom and A. Fridman, (1988).
24. M. Sands, SLAC-PUB 121, (1970). See equation 5.85.